International Journal of Fluid Machinery and Systems
Vol. 5, No. 1, January-March 2012

DOI: http://dx.doi.org/10.5293/IJFMS.2012.5.1.038
ISSN (Online): 1882-9554

**Original Paper**

# Performance Prediction of Centrifugal Compressor Based on Performance Test, Similarity Conversion and CFD Simulation

**Changyun Zhu and Guoliang Qin**

School of Energy and Power Engineering, Xi'an Jiaotong University University
No.28, Xianning West Road, Shaanxi, 710049, P.R. China, zcysxj@gmail.com, glqin@mail.xjtu.edu.cn

**Abstract**

One centrifugal compressor is applied for refrigeration and its working substance is R134a. The operating points obtained by using similar conversion at different rotation speeds are compared with the numerical results. They keep consistent with each other while the rotation speeds are lower, but the error between them will become large with the increasing of the rotation speed. Then the operating points are obtained when the working substance is air by using two similar conversion methods separately. Based on the comparison, it can be obtained that the result of keeping the specific volume ratio of inlet and outlet is more accurate than the result of maintaining Ma number. Then the test result is compared with the similarity result and the numerical result when the working substance is air. It is obtained that the similarity result is more consistent with the test result better than the numerical result and the trend of efficiency and pressure ratio change with the flow rate is consistent with the test result. In the process of similar conversion, the efficiency η is no useful for similitude design and it has less influence on the conversion result.

**Keywords:** Similitude design, similar conversion, centrifugal compressor

## 1. Introduction

In the industry field, the kinds of the centrifugal compressor's working substance are increasing more and more, such as hydrogen[1],oxygen[2], carbon dioxide[3], R134a[4-6], and mixture of several gases[7]. How to obtain the performance of the centrifugal compressor economically and accurately is attractive for researchers [8, 9] when the working substance is real gas.

The centrifugal compressor is used for central air conditioning system widely and R134a is its working substance, such as in [10]. Zhiheng Wang [11] has studied the aspect of the gas model for the numerical simulation result and obtained that the result by using real gas model is more accurate.

The performance test of centrifugal compressor was carried on in [12, 13] as R134a is applied. But the test is very expensive. It needs to establish closed test bench which including chiller, boiler and valves.

It is economic and convenient to predict the performance of centrifugal compressor using numerical method[14, 15].The similar conversion method is also applied to predict the performance of centrifugal compressor, such as the affect of the specific heat ratio on the aerodynamic performance of turbomachinery is studied in [16], the centrifugal compressor design method based on the similarity is studied in [17,18],the influence of geometric scaling on the stability and range of centrifugal compressor is studied in [19].

In this study, the test result is obtained on the open test bench when the working substance is air. By using similar conversion, the performance of the centrifugal compressor is obtained when the working substance is R134a. But if the relative Ma number is greater than the threshold, the similar conversion result will be no longer applicable. So the numerical simulation is applied to judge whether the Ma number is greater than the critical Ma number firstly.

## 2. Design Parameters of the Centrifugal Compressor

Vaneless diffuser and semiclosed-type impeller is applied for the centrifugal compressor. The geometric data and design specification of the centrifugal compressor is shown in Tab.1. The impeller's 3D model is shown in Fig.1.

Received October 31 2011; accepted for publication November 13 2011: Review conducted by Prof. Yulin Wu. (Paper number O11023C)
Corresponding author: Changyun Zhu, Professor, zcysxj@gmail.com

**Table 1** Geometric data and design specification of the centrifugal compressor

| Design specifications | |
|---|---|
| Rotation speed of machine | n=14515rpm |
| Inlet pressure | P1=360000Pa |
| Inlet temperature | T1=280.15K |
| Mass flow | qm=14.58kg/s |
| Outlet pressure | P2=939600Pa |
| Geometrical specifications | |
| Diameter of impeller's inlet | D1=150mm |
| Diameter of impeller's outlet | D2=260mm |
| Width of impeller's outlet | b2=15mm |
| Angle of impeller's outlet | β2A =50° |
| Diameter of diffuser's inlet | D3=264 mm |
| Diameter of diffuser's outlet | D4=420 mm |
| Width of diffuser | b3=b4=15 mm |

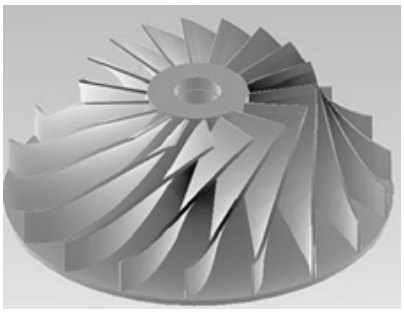

**Fig. 1** 3D model of the impeller

## 3. Numerical Simulation for the Centrifugal Compressor

### 3.1 Mesh of the Volute and Diffuser

The mesh of the volute is shown in Fig. 2. The connections between the blocks can introduce numerical error, so only 6 blocks are used. The butterfly mesh is used for each block to improve the mesh's orthogonality. The butterfly topology for outlet of the volute is shown in Fig. 3. In order to reduce the numerical error of the connections, the mesh topology of the connective faces is kept consistent with each other.

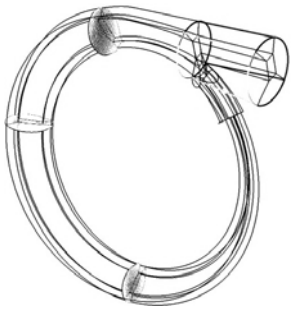

**Fig. 2** Blocks of the volute mesh

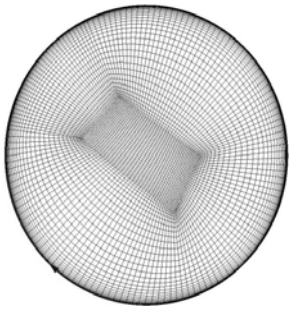

**Fig. 3** Butterfly topology for outlet of the volute

The mesh of the vaneless diffuser is divided as 4 blocks. The mesh of stator includes the mesh of volute and vaneless diffuser. Coarser grid of the stator mesh is shown in Fig. 4. The number of the mesh's total nodes is 3575451.

### 3.2 Mesh of the Stage

The mesh of the stage is shown in Fig. **4** Coarser grid of the stator mesh **Fig. 5**, it includes impeller, vaneless diffuser and volute. The rotor/stator interface is located between the outlet of impeller and inlet of the vaneless diffuser. The minimum value of orthogonality is 8.24 which can keep the numerical result is no sensitive to the mesh.

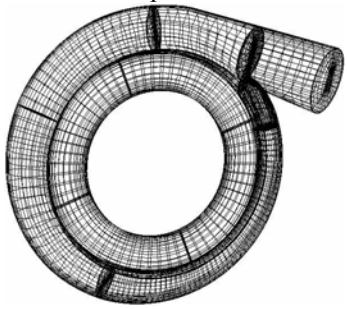

**Fig. 4** Coarser grid of the stator mesh

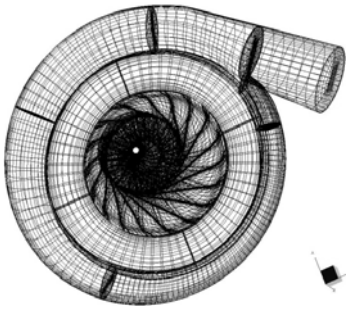

**Fig. 5** Coarser mesh of the stage

### 3.3 Setting of the Numerical Simulation

Real gas model is used in the numerical simulation when the working substance is air or R134a. Frozen rotor method is used for Rotor/stator coupling. The total temperature, total pressure and flow direction is given at the inlet of impeller. Mass flow rate and initial pressure is given at the outlet of the volute. The applied turbulence model is Spalart-Allmaras model.

## 4. Similar Conversion when the Working Substance is R134a at Different Rotation Speed and Numerical Result

For the same machine, when its inlet conditions are kept unchanged and working substance is the same one, the performance parameters at the different rotation speeds can be obtained by similar conversion. It is generally considered that the change of the Ma number has less influence on the parameters of the flow path and resistance coefficients, such as $\beta_{df}$ and $\beta_l$. Then the influence of Ma number can be neglected. The Ma number can be expressed as follows,

$$Ma_{2u} = \frac{u_2}{\sqrt{\kappa R T_{in}}} \tag{1}$$

### 4.1 Pressure Ratio Relation

The relation of inlet flow coefficient can be deduced from similarity of inlet velocity triangles

$$\varphi_1' = \varphi_1 \tag{2}$$

$$\frac{q_{Vin}'}{n'} = \frac{q_{Vin}}{n} \tag{3}$$

Similarly, because of the similarity of outlet velocity triangles,

$$\varphi_{2r}' = \varphi_{2r} \tag{4}$$

$$\varphi_{2u}' = \varphi_{2u} \tag{5}$$

Because of $\beta_{df}$ and $\beta_l$ keeps unchanged then the efficiency satisfy Eq.6,

$$\eta_{pol}' = \eta_{pol}, m' = m \tag{6}$$

The $\eta$ is defined as follows,

$$\eta = \eta_{pol} = \frac{1}{\frac{\kappa}{\kappa-1}} \frac{\lg\left(\frac{p_2}{p_1}\right)}{\lg\left(\frac{T_2}{T_1}\right)} \tag{7}$$

From Eq. (4), the energy head coefficient satisfy the follows Eq.8,

$$\phi_{pol}' = \phi_{pol} \tag{8}$$

Then the energy head relation satisfy the follows

$$\frac{h_{pol}'}{h_{pol}} = \frac{\phi_{pol}' u_2'^2}{\phi_{pol} u_2^2} = \frac{u_2'^2}{u_2^2} = \frac{n'^2}{n^2} \tag{9}$$

The energy head relation

$$h_{pol}' = \frac{m'}{m'-1} R'T' \left( \varepsilon'^{\frac{m'}{m'-1}} - 1 \right) \tag{10}$$

$$h_{pol} = \frac{m}{m-1} RT \left( \varepsilon^{\frac{m}{m-1}} - 1 \right) \tag{11}$$

The pressure ratio relation

$$\varepsilon' = \left[ 1 + \left( \frac{n'}{n} \right)^2 \frac{RT_{in}}{R'T_{in}'} \left( \varepsilon^{\frac{m-1}{m}} - 1 \right) \right]^{\frac{m'}{m'-1}} \tag{12}$$

### 4.2 The Inlet Volume Flow Rate Relation

Assuming that at a certain section of the compressor flow path，the speed triangles are similar to each other and the volume flow of the section is $q_{Vm}$. Then

$$\frac{q'_{Vm}}{n'} = \frac{q_{Vm}}{n} \tag{13}$$

Assuming that

$$\frac{q_{Vm}}{q_{Vin}} = \frac{\upsilon_m}{\upsilon_{in}} = \frac{1}{K_{Vm}} \tag{14}$$

$$\frac{q'_{Vm}}{q'_{Vin}} = \frac{\upsilon'_m}{\upsilon'_{in}} = \frac{1}{K'_{Vm}} \tag{15}$$

It can be obtained that

$$q'_{Vin} = q_{Vin} \frac{n'}{n} \frac{K'_{Vm}}{K_{Vm}} \tag{16}$$

The inlet volume flow rate relation

$$q'_{Vin} = q_{Vin} \frac{n'}{n} \frac{K'_{Vm}}{K_{Vm}} \tag{17}$$

According to some experiment data, it can be obtained that

$$\frac{K'_{Vm}}{K_{Vm}} = \frac{\sqrt{\left(1+\frac{\Delta T'}{2T'_{in}}\right)^{\frac{1}{m'-1}}}}{\sqrt{\left(1+\frac{\Delta T}{2T_{in}}\right)^{\frac{1}{m-1}}}} \tag{18}$$

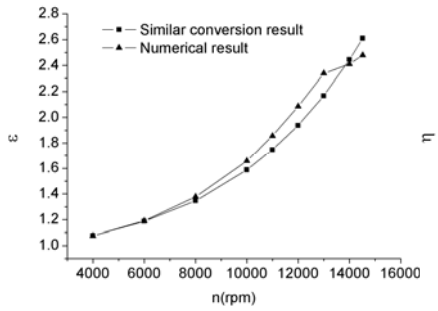


**Fig. 6** Comparison of **ε**

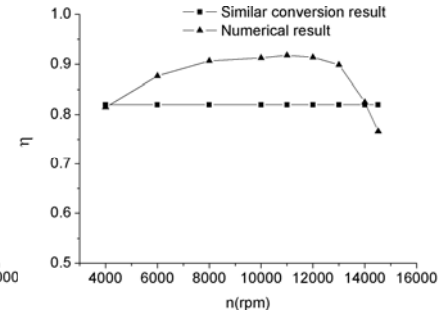


**Fig. 7** Comparison of η

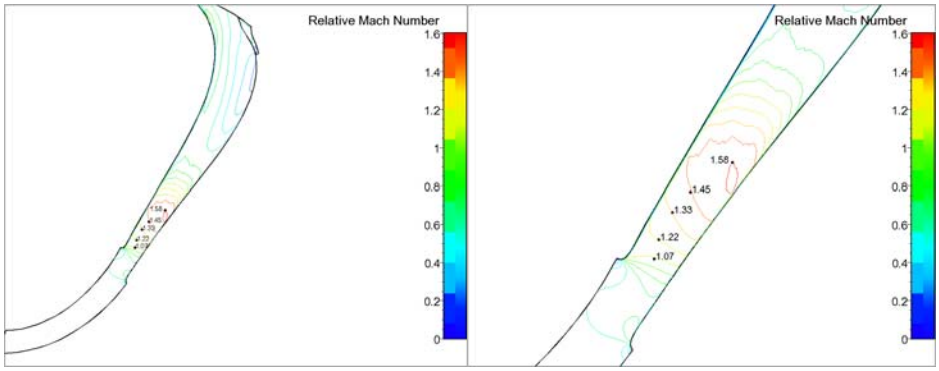


**Fig. 8** The relative Mach number in the flow path n=14515rpm

The numerical results and similarity results at the different rotation speeds are compared in Fig. 6 and their mass flow rates are kept the same with each other at the same rotation speed.

It can be obtained that the error between the two ε is very less while the rotation speed is lower. When the rotation speed is higher than n=10000rpm, the error between them becomes larger with the increasing of the rotation speed.

When the rotation speed n=14000rpm and n=14515rpm, the ε break its trend and they are smaller than the similarity results. It is because the relative Mach number in the flow path is greater than the threshold of the Mach number, in fact it is impossible. Blocking appears in the flow path when n>14000rpm and the efficiency also drops down in Fig. 7. When blocking appears in the flow path, the similarity law is failure. Fig. 8 shows the relative Mach number in the flow path when n=14000rpm and the working substance is R134a, it can be obtained that the relative Mach number>1 and it can be concluded that the flow blocking appear in the flow path.

The efficiency of numerical result is lower than the similarity result when n=4000rpm, it perhaps because that the Re=$\frac{u_2 D_2}{\nu}$ =1.2×10$^6$ is lower than the critical Re and the friction loss accounts for a large proportion of total energy. In fact, the efficiency η has a small influence on the similarity results.

So it can obtained that the similarity conversion is suit for the situation that the Re is greater than critical Re and the Mach number is smaller than the critical Mach number. The error between them increases with the increasing of rotation speed.

## 5. Similar Conversion When the Adiabatic Index is Unequal to Each Other

In the following work, the design operating point of the machine when its working substance is R134a is similarly conversed to the corresponding operating point when its working substance is air. The numerical result, the testing result and the similarity result are compared with each other.

The adiabatic index κ is different between the R134a and air. There are two similar conversion methods and their results are compared.

### 5.1 Similarity Conversion Method by Keeping the Specific Volume Ratio of Inlet and Outlet

In this study, it is called as the first similarity conversion method. This similar conversion method is by keeping the specific volume ratio of inlet and outlet as follows

$$\frac{\upsilon'_{in}}{\upsilon'_{out}} = \frac{\upsilon_{in}}{\upsilon_{out}} \tag{19}$$

The pressure ratio relation can be deduced

$$\varepsilon'^{\frac{1}{m'}} = \varepsilon^{\frac{1}{m}} \tag{20}$$

Because of the similarity of the machine, assuming that

$$\eta'_{pol} = \eta_{pol}, \eta'_{hyd} = \eta_{hyd} \tag{21}$$

The energy head coefficient relation

$$\phi'_{pol} = \phi_{pol} \tag{22}$$

The energy head relation

$$h'_{pol} = \left(\frac{n'}{n}\right)^2 h_{pol} \tag{23}$$

The rotation speed relation

$$\begin{aligned} n' = n_{eq} &= n\sqrt{\frac{h'_{pol}}{h_{pol}}} = n\sqrt{\frac{\frac{m'}{m'-1}R'T'_{in}\left[\left(\varepsilon'\right)^{\frac{m-1}{m}}-1\right]}{\frac{m}{m-1}RT_{in}\left[\left(\varepsilon\right)^{\frac{m-1}{m}}-1\right]}} \\ &= n\sqrt{\frac{\frac{m'}{m'-1}R'T'_{in}\left[\left(\frac{\upsilon'_{in}}{\upsilon'_{out}}\right)^{\frac{m-1}{m}}-1\right]}{\frac{m}{m-1}RT_{in}\left[\left(\frac{\upsilon_{in}}{\upsilon_{out}}\right)^{\frac{m-1}{m}}-1\right]}} \end{aligned} \tag{24}$$

The inlet volume flow rate relation

$$q'_{Vin} = \frac{n'}{n} q_{Vin} \tag{25}$$

When the rotation speed is n=14515rpm and the working substance is R134a, it can be obtained from Eq. (8) that the rotation speed of the corresponding similar operating point is n'=41003rpm. The impeller's critical speed is about $n_c$=25000rpm from the result of dynamics analysis and the impeller only can rot at the speed below n'=25000rpm. So it need to obtained the machine's

performance at the lower speed when its working substance is R134a by similar conversion method introduced in section 4, then obtain the corresponding similarity operating point at the speed below n'=25000rpm when its working substance is air by similar conversion.

The similar conversion results at different rotation speeds are shown in Tab. 2 while the working substance is air.

**Table 2** Similarity result at different speeds

| | | | | |
|---|---|---|---|---|
| $T_1$ | 304.35 | 307.26 | 306.45 | 306.74 |
| n | 15000 | 17500 | 20000 | 22500 |
| $P_1$ | 96300 | 96800 | 96790 | 96300 |
| $q_{vin}$ | 42.6 | 50.4 | 58.2 | 66.6 |
| ε | 1.256 | 1.354 | 1.479 | 1.626 |
| η | 0.82 | 0.82 | 0.82 | 0.82 |

### 5.2 Similarity Conversion Method by Maintaining the Ma Number

This similar conversion method is called the second similar conversion method in this study. When the Ma number is high, it affects the flow significantly, so maintaining the same size of Ma number is important to ensure the similarity. But it is impossible to keep the Ma number equal with each other at the corresponding points of the flow paths because of κ≠κ', such as when keeping $Ma_{2u}=Ma'_{2u}$, but $Ma_{2c}\neq Ma'_{2c}$, $Ma_{2w}\neq Ma'_{2w}$。.

It is supposed that keeping $Ma_{2c}=Ma'_{2c}$ can keep the machine's similarity, and considering the relation of inlet Ma number, the relation of $Ma_{2u}$ can be obtained as the follows.

According to the speed triangle

$$c_2^2 = c_{2r}^2 + c_{2u}^2 = (\varphi_{2r}^2 + \varphi_{2r}^2)u_2^2 \tag{26}$$

So it can be obtained that

$$Ma_{2u} = \frac{u_2}{\sqrt{\kappa R T_{in}}}, Ma_{2c} = \frac{c_2}{\sqrt{\kappa R T_{in}}} \tag{27}$$

$$Ma_{2c}^2 = (\varphi_{2r}^2 + \varphi_{2r}^2) Ma_{2u}^2 \frac{T_{in}}{T_2} \tag{28}$$

$$Ma_{2c} = Ma\sqrt{(\varphi_{2r}^2 + \varphi_{2r}^2)\frac{T_{in}}{T_2}} \tag{29}$$

According to the energy equation

$$h_{tot} = W_{tot} = c_p(T_2 - T_{in}) + \frac{c_2^2 - c_{in}^2}{2} \tag{30}$$

By assuming that

$$c_{in}^2 = 0$$

Then it can be obtained that

$$T_{in}\left(\frac{T_2}{T_{in}} - 1\right) = \frac{\kappa - 1}{\kappa R} h_{tot}\left(1 - \frac{c_2^2}{2h_{tot}}\right) \tag{31}$$

Because

$$h_{tot} = \phi_{tot} u_2^2, \quad \frac{c_2^2}{2h_{th}} = 1 - \rho \tag{32}$$

Let

$$1 - \Omega = \frac{1 - \rho}{1 + \beta_{df} + \beta_l} \tag{33}$$

$$\Omega = 1 - \frac{\varphi_{2u}}{2} \tag{34}$$

With Eq. (29), it can be obtained that

$$\frac{T_2}{T_{in}} = 1 + \Omega(\kappa - 1)\phi_{tot} M'_{2u} \tag{35}$$

It can be obtained that

$$Ma_{2c} = Ma_{2u}\sqrt{\frac{(\varphi_{2r}^2 + \varphi_{2r}^2)}{1 + \Omega(\kappa - 1)\phi_{tot} Ma_{2u}^2}} \tag{36}$$

$$Ma_{1w} = Ma_{2u}\sqrt{\frac{T_{in}}{T_1}\left(\left(\frac{c_1}{u_2}\right)^2 + \left(\frac{D_1}{D_2}\right)^2\right)} \tag{37}$$

$$Ma'_{2u}\sqrt{\frac{(\varphi'^2_{2r} + \varphi'^2_{2r})}{1+\Omega'(\kappa'-1)\phi'_{tot}Ma'^2_{2u}}} = Ma_{2u}\sqrt{\frac{(\varphi^2_{2r} + \varphi^2_{2r})}{1+\Omega(\kappa-1)\phi_{tot}Ma^2_{2u}}} \tag{38}$$

$$Ma'_{2u} = \frac{1}{2}Ma_{2u}\left(1 + \frac{1}{\sqrt{1-\Omega(\kappa'-\kappa)\phi_{tot}Ma_{2u}}}\right) \tag{39}$$

The rotation speed relation

$$n_{eq} = \frac{1}{2}\left(1 + \frac{1}{\sqrt{1-\Omega(\kappa'-\kappa)\phi_{tot}Ma_{2u}}}\right)\sqrt{\frac{\kappa R'T'_{in}}{\kappa RT_{in}}}n \tag{40}$$

For the similarity of inlet velocity triangles

$$\varphi_{2r} = \varphi'_{2r} \tag{41}$$

It can be obtained that

$$\frac{q_{V2}}{u_2} = \frac{q'_{V2}}{u'_2} \tag{42}$$

$$\frac{\rho_2}{\rho_{in}} = \left[1+\Omega(\kappa-1)\phi_{tot}Ma^2_{2u}\right]^{\frac{1}{m-1}} \tag{43}$$

It can be obtained that

$$q'_{Vin} = q'_{V2}\frac{\rho'_2}{\rho'_{in}} = q'_{V2}\left[1+\Omega'(\kappa'-1)\phi'_{tot}Ma'^2_{2u}\right]^{\frac{1}{m'-1}} \tag{44}$$

$$q_{Vin} = q_{V2}\frac{\rho_2}{\rho_{in}} = q_{V2}\left[1+\Omega(\kappa-1)\phi_{tot}Ma^2_{2u}\right]^{\frac{1}{m-1}} \tag{45}$$

The inlet volume flow rate relation

$$q'_{Vin} = q_{Vin}\frac{u'_2}{u_2}\frac{\left[1+\Omega'(\kappa'-1)\phi'_{tot}Ma'^2_{2u}\right]^{\frac{1}{m'-1}}}{\left[1+\Omega(\kappa-1)\phi_{tot}Ma^2_{2u}\right]^{\frac{1}{m-1}}} \tag{46}$$

The similar conversion results by the second method at different speeds while the working substance is air are shown in Tab. 3.

**Table 3** Similarity result at different speeds

| | | | | |
|---|---|---|---|---|
| $T_1$ | 304.35 | 307.26 | 306.45 | 306.74 |
| n | 15000 | 17500 | 20000 | 22500 |
| $P_1$ | 96300 | 96800 | 96790 | 96300 |
| $q_{vin}$ | 60.18 | 60.24 | 60.24 | 60.3 |
| ε | 1.413 | 1.58 | 1.802 | 2.070 |
| η | 0.82 | 0.82 | 0.82 | 0.82 |

In Fig. 9, the volume flow rates of the two conversion methods and the test result are compared, it can be obtained that the volume flow rates of the first conversion method and the test obey the same law approximately, despite the value of test at n=20000rpm deviates from the law. But the volume flow rates of the second conversion method obey one wrongr law. So in the follows, if the conversion method is referred, the conversion method will be the first conversion method.

In Fig. 10, the ε of the first conversion method is consistent with the test result well but the ε of the second conversion method doesn't match well with the test result.

In Fig. 11, the η of the two conversion methods and the test result have big error. The η of the test is lower than the design object and increases with the rotation speed increase.

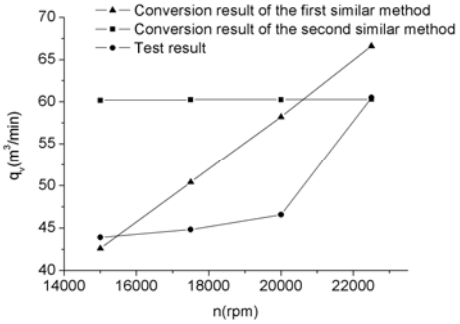


**Fig. 9** Comparison of volume flow rates

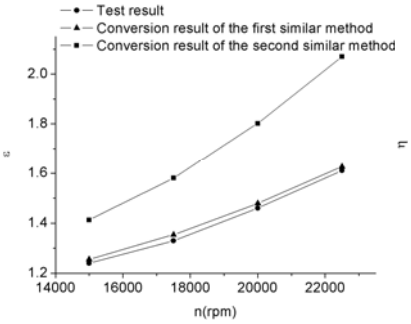


**Fig. 10** Comparison of ε

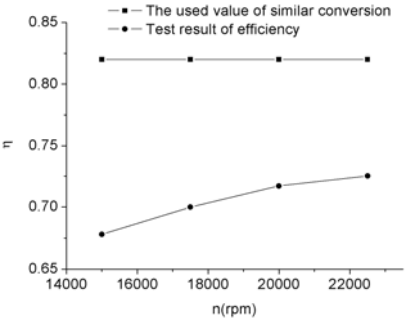


**Fig. 11** Comparison of η

From the comparison between volume flow rate, ε and η, it can be obtained that the ε of the first conversion method is very accurate and the η as an input parameter in the process of similitude conversion has small influence on the conversion result.

## 6. Test Bench and Test Result

The performance test is preceded at a series speeds in aerodynamics center of Xi'an Jiaotong University. The style of the test bench is open and the working substance is air. The pictures of test bench are Fig. 12 and Fig. 13. The measurement plane positions are assigned according to the regulations of PTC-10.

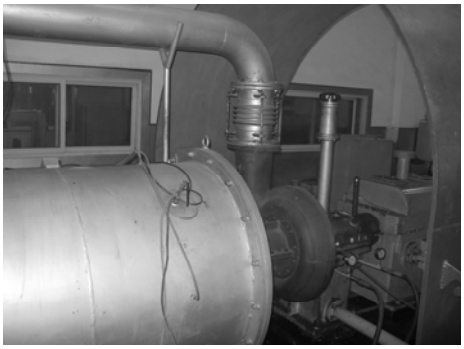

**Fig. 12** Test bench of the centrifugal compressor

**Fig. 13** Test bench of the centrifugal compressor

### 6.1 Test Result

The relation curves of the inlet volume flow rate and pressure ratio obtained from the test result at the deferent rotation speeds are shown in Fig. 14. Fig. 15 shows the relation curves of the inlet volume flow rate and η at deferent rotation speeds.

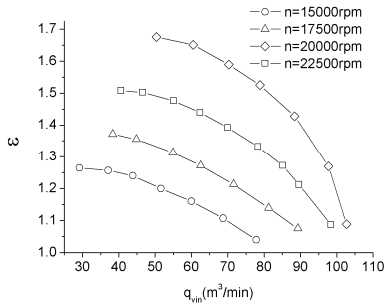


**Fig. 14** The relation curves of the inlet volume flow rate and ε at deferent rotation speeds

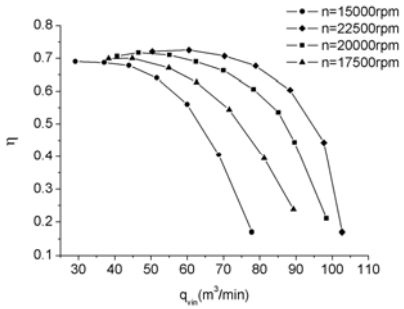


**Fig. 15** The relation curves of the inlet volume flow rate and η at deferent rotation speeds

### 6.2 Comparison between the Numerical Result, Similar Conversion Result and Test Result

The numerical result, test result and similar conversion result are compared from Fig. 16 to Fig. 23. It can be obtained that the error between the numerical result and the test result is bigger than the error of between the similar conversion result and the

test result.

In this computation case, the leakage is not included. The geometry of computation is not consistent with the real test bench, such as the geometry doesn't include the inlet pipe and outlet pipe. The above two points bring error for computation. The trend of η and ε change with the flow rate is consistent with the test result.

The operating points of the machine when the working substance is R134a at the rotation speed n=14515rpm is obtained by using the similarity method of keeping the specific volume ratio of inlet and outlet and is shown in Fig. 24. The design operating point is located between the curves of computational result and similar conversion result.

From Fig. 25, it can be obtained that the numerical result and the used value in the similar conversion has difference. In fact the used value in the similar conversion is the test result. It also can be obtained as the above that the η as an input parameter in the process of similitude conversion has small influence on the conversion result.

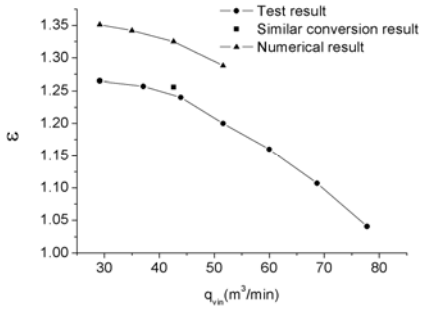


**Fig. 16** Comparison of the ε at n=15000rpm

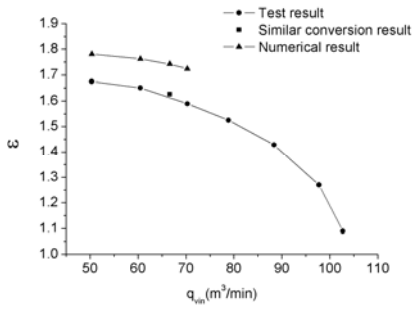


**Fig. 17** Comparison of the ε at n=22500rpm

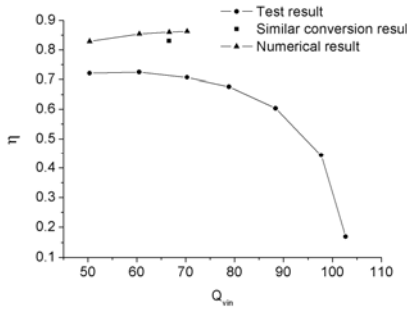


**Fig. 18** Comparison of the η at n=22500rpm

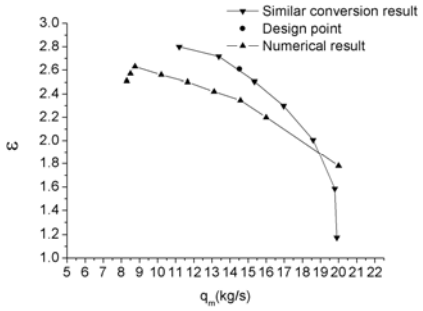


**Fig. 19** Comparison of ε

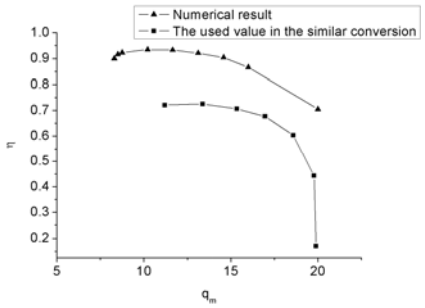


**Fig. 20** Comparison of η of the used value in similar conversion, the numerical result when the working substance is R134a

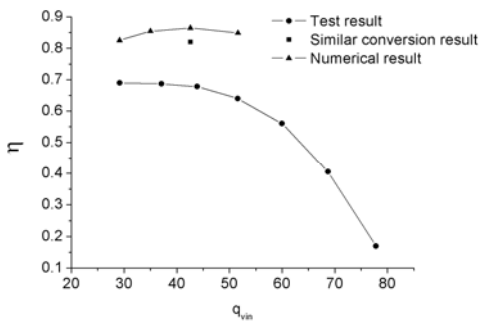


**Fig. 21** Comparison of the η at n=15000rpm

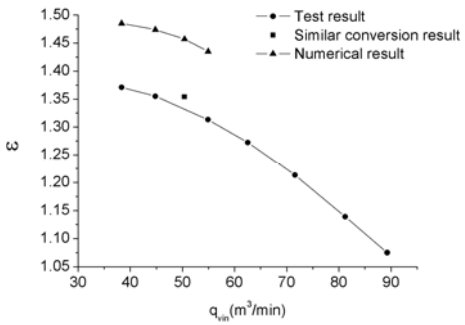


**Fig. 22** Comparison of the ε at n=17500rpm

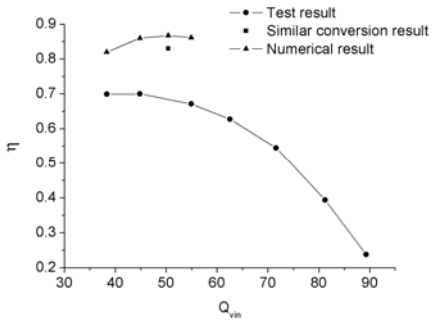


**Fig. 23** Comparison of the η at n=17500rpm

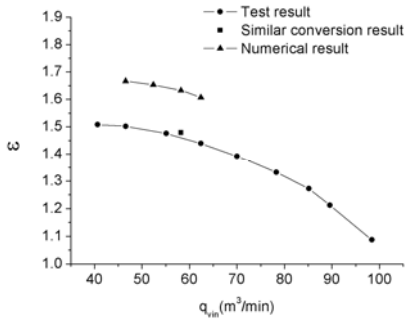


**Fig. 24** Comparison of the ε at n=20000rpm

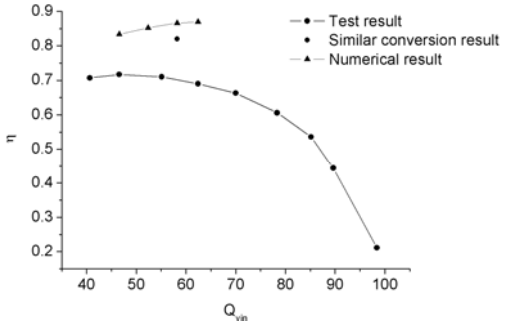


**Fig. 25** Comparison of the η at n=20000rpm

## 7. Conclusions

In this manuscript, by comparison of the result of the two similar conversion methods when the adiabatic index is unequal to each other, it can be obtained that the result obtained from the similarity conversion method by keeping the specific volume ratio of inlet and outlet is more accurate than the similarity conversion method of maintaining the Ma number.

In the similitude design process when the working substance is R134a, if the performance of compressor is obtained by convert the test result using air, numerical simulating is ought to be used for decide if the Ma number reach the critical value. If the Ma number reaches the critical value, the similar conversion method will not be fit to be applied.

The pressure ratio ε obtained by similar conversion can be used as reference value. The efficiency η is no useful and its change has small influence on the conversion result.


## Acknowledgments

The authors wish to thank for many engineers and colleagues for their assistance and useful discussions, which made this work possible.


## Nomenclature

| | | | |
|---|---|---|---|
| $h_{pol}$ | The total energy head | $Ma_{2u}$ | Mach number of peripheral velocity of impeller |
| m | Polytropic exponent | κ | Adiabatic index |
| R | Gas constant | $\Omega = 1 - \frac{\varphi_{2u}}{2}$ | Reaction degree |
| ε | Pressure ratio | $\phi_{tot}$ | The total energy head coefficient |
| $q_{Vin}$ | Inlet volume flow rate | $Ma_{2c}$ | Absolute Mach number at outlet of impeller |
| $K_{Vm} = \frac{q_{Vin}}{q_{Vm}}$ | Specific volume | $\varphi_{2u} = \frac{c_{2u}}{u_2}$ | Flow coefficient |

## References


[1] Lei, Z., Dipjyoti, A., Jayanta, K., Louis, C., Nagaraj, A., 2007, "Aerodynamics performance test of a high-speed miniature centrifugal compressor," ASME Paper ES2007-36212.

[2] Ahmed, A., 2005, "Design of a moderate speed-high capacity centrifugal compressor with application to PSA and VPSA air separation processes," ASME Paper PWR2005-50140.

[3] Roberts, SK., Sjolander, SA., 2002, "Semi-Closed Cycle O2/CO2 Combustion Gas Turbines: Influence of Fluid Properties on the Aerodynamic Performance of the Turbomachinery," ASME Paper GT2002-30410.

[4] Aida, Y., Shimizu, I., Tomizawa, H., Kobayashi, K., Asakura, H., Kouki, T., Kimijima, T., Nogaku, T., 1996 "Development of R134a centrifugal water chiller," Ishikawajima-Harima Giho/IHI Engineering Review, 36, No. 4, pp. 321-325.

[5] Schiffmann, J., Favrat, D., 2009, "Experimental investigation of a direct driven radial compressor for domestic heat pumps," International Journal of Refrigeration, 32, No. 8, pp. 1918-1928.

[6] Aprea, C., 2002, "A zero ODP replacement for R12 in a centrifugal compressor: An experimental study using R134a," International Journal of Energy Research, 26, No. 15, pp. 1323-1331.

[7] Øyvind, H., Bakken, LE., Grüner, TG., Lars, B., Tor, B., 2008, "Wet Gas Performance of a Single Stage Centrifugal Compressor," ASME Paper GT2008-51156.

[8] Ruitao, L., Zhong, X., 2004, "Numerical investigation to the flow of real gas in a centrifugal compressor," Journal of Xi'an Jiaotong University, 38, No. 3, pp. 317-321.

[9] Nakagawa, K., S, Tanaka., J, Kaneko., 1992, "An aerodynamic investigation of a centrifugal compressor for HCFC123," International Journal of Refrigeration, 15, No. 4, pp. 199-205.

[10] Junjie, G., Masahiro, K., Tracey, SP., James, C., 2003, "Multi-Channel R134a Two-Phase Flow Measurement Technique for Automobile Air-Conditioning System," ASME Paper FEDSM2003-45379.

[11] ZhiHeng, W., Guang, X., 2008, "The effects of gas models on the predicted performance and flow of a centrifugal refrigeration compressor stage," Sciencein China Series E: Technological Sciences, 51, No. 8, pp 1160-1168.

[12] Schiffmann, J., Favrat, D., 2009, "Experimental investigation of a direct driven radial compressor for domestic heat pumps," International Journal of Refrigeration, 32, No. 8, pp. 1918-1928.

[13] Aprea, C., 2002, "A zero ODP replacement for R12 in a centrifugal compressor: An experimental study using R134a," International Journal of Energy Research, 26, No. 15, pp. 1323-1331.

[14] Michele M, Filippo R., Andrea A., Seiichi I., 2008, "Design and Off-Design Numerical Investigation of a Transonic Double-Splitter Centrifugal Compressor," ASME Paper GT2008-50759.

[15] Barton, MT., Mansour, ML., Liu, JS., Palmer, DL., 2006, "Numerical Optimization of a Vaned Shroud Design for Increased Operability Margin in Modern Centrifugal Compressors," ASME Paper GT2004-54287.

[16] Roberts, SK., Sjolander, SA., 2005, "Effect of the Specific Heat Ratio on the Aerodynamic Performance of Turbomachinery," Journal of Engineering for Gas Turbines and Power , 127, No. 4, pp. 773-780.

[17] Den, GN., Malyshev, AA., 2004, "Modeling of the Flow Parts of Stationary Centrifugal Compressor Machines for Compression of Real Gases. Gasdynamic Tests and Processing of Their Results. I. Theoretical Calculations," Journal of Engineering Physics and Thermophysics, 75, No. 5, pp. 1076-1085.

[18] Guillaume, D., Xavier C., Jean-Bernard C., Patrick C., 2006, "Practical Use of Similarity and Scaling Laws for Centrifugal Compressor Design," ASME Paper GT2006-91227.

[19] Matthias S., Abhari, RS., 2005, "Influence of geometric scaling on the stability and range of a turbocharger centrifugal compressor," ASME Paper GT2005-68713.

[20] Zhong, X, 1978 "The fundamental theory of centrifugal compressor," Machinery Industry Press, Beijing, pp. 117-127, Chap.6.